LUND UNIVERSITY

Quantitative aspects on myocardial perfusion scintigraphy

Senneby, Martin

2023

Document Version:
Publisher's PDF, also known as Version of record

Quantitative Aspects on Myocardial Perfusion Scintigraphy

MARTIN SENNEBY
DEPARTMENT OF TRANSLATIONAL MEDICINE | LUND UNIVERSITY

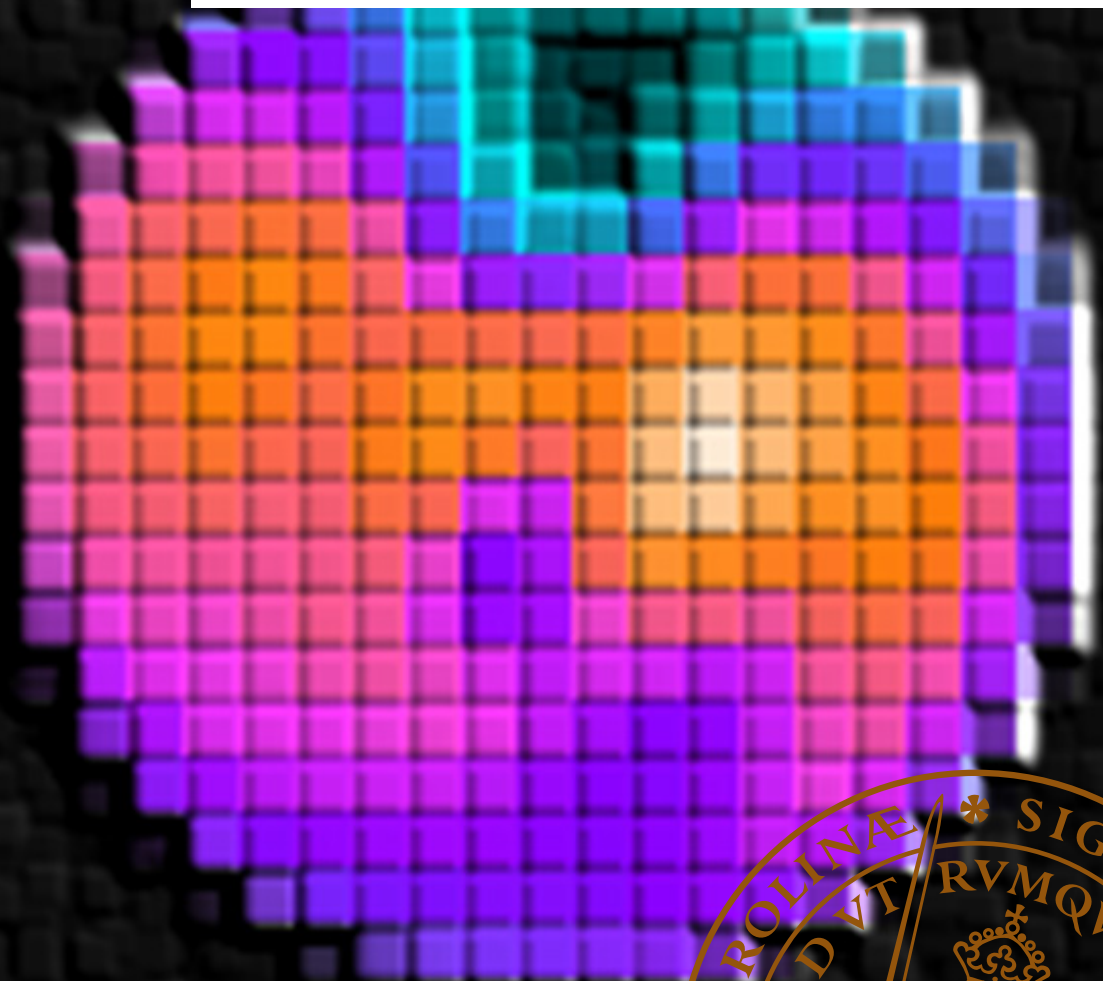

Quantitative Aspects on Myocardial Perfusion Scintigraphy

Martin Senneby

LUND
UNIVERSITY

DOCTORAL DISSERTATION

Doctoral dissertation for the licentiate degree at the Faculty of Medicine at Lund University to be publicly defended on the 9th of March at 09.00 in room 2007, Department of Medical Imaging and Physiology, Cark Bertil Laurells gata 9, Skåne University Hospital, Malmö.

Faculty opponent
MD, PhD Thomas Larsson, Karolinska Institute

Organization LUND UNIVERSITY Faculty of Medicine Department of Translational Medicine Clinical Physiology and Nuclear Medicine	**Document name** Doctoral dissertation **Date of issue** 2023-03-09
Author Martin Senneby	Sponsoring organization

Title and subtitle

Quantitative Aspects on Myocardial Perfusion Scintigraphy

Abstract

Background

Ischemic heart disease (IHD) remains the leading cause of death worldwide. Cardiac imaging plays a vital role in diagnosing IHD. One such method is myocardial perfusion scintigraphy (MPS), which is established and widely used. MPS uses single-photon emission computed tomography (SPECT) to acquire three-dimensional images of the myocardial perfusion.

Aim

The aim of this thesis was to explore quantitative aspects regarding MPS to possibly improve and facilitate interpretation. The first study introduce and validate the concept of the perfusion vector and its potential to assist visual interpretation of MPS examinations. The second study compare the IQ-SPECT camera system with a conventional SPECT camera in regard to perfusion data and left ventricular function. The IQ-SPECT camera system uses a multifocal collimator that increases sensitivity, compared to the parallel hole collimator used in conventional SPECT.

Methods

In the first study the perfusion vector is introduced as the difference between the anatomical centroid (in this case the left ventricle) and the perfusion center of gravity. The perfusion vector was tested in both simulated and in patient MPS images. Simulated images were created with various perfusion defect sizes and locations. Patient studies included both normal and abnormal (with specific perfusion defects) images. In the second study, patients were examined with both the IQ-SPECT camera system and the conventional SPECT camera.

Results

The perfusion vector behaved as expected in simulated images, with the vector pointing away from perfusion defects. When tested on patient images the vector magnitude was small for the normal group while changing direction in mostly the expected way for the abnormal group. A correlation was found between vector size and defect extent. When comparing the IQ-SPECT with conventional SPECT similar mean values were found for perfusion data while left ventricular volumes were lower and left ventricular ejection fraction (EF) was higher for IQ-SPECT acquisitions.

Conclusions

The perfusion vector was shown to have potential in assisting the visual interpretation of MPS examinations. The small vector magnitude in normal patients could be used to decide if an examination is normal or not.

No major differences in the interpretation of MPS studies regarding perfusion data can be expected between the IQ-SPECT system and a conventional SPECT system. However, cardiac volumes were lower and EF higher for IQ-SPECT, which should be further investigated using a reference method.

Key words

Myocardial Perfusion Scintigraphy, SPECT, Quantification, Ischemic Heart Disease.

Classification system and/or index terms (if any)

Supplementary bibliographical information		**Language** English
ISSN and key title 1652-8220		**ISBN** 978-91-8021-384-4
Recipient's notes	**Number of pages** 45	Price
	Security classification	

Signature  Date 2023-01-20

Quantitative Aspects on Myocardial Perfusion Scintigraphy

Martin Senneby

LUND
UNIVERSITY

Faculty of Medicine, Lund University
Department of Translational Medicine

ISBN 978-91-8021-384-4
ISSN 1652-8220

Printed in Sweden by Media-Tryck, Lund University
Lund 2023

To my family

Table of Contents

List of papers

This thesis is based on the following papers, which are referenced in the text by their Roman numerals.

I. Minarik D, **Senneby M**, Wollmer M, Mansten A, Sjöstrand K, Edenbrandt L, Trägårdh E. Perfusion vector – a new method to quantify myocardial perfusion scintigraphy images: a simulation study with validation in patients. EJNMMI Research 2015; 5:42

II. **Senneby M**, Minarik D, Wollmer P, Trägårdh E. Quantitative parameters in myocardial perfusion scintigraphy: comparison between dedicated multifocal collimators and standard parallel hole collimators. Manuscript.

Abbreviations

AC	Attenuation correction
ACS	Acute coronary syndrome
CAD	Coronary artery disease
CCS	Chronic coronary syndrome
CCTA	Coronary computed tomography angiography
CT	Computed tomography
ECG	Electrocardiography
EDV	End-diastolic volume
EF	Ejection fraction
ESV	End-systolic volume
FBP	Filtered back projection
FFR	Fractional flow reserve
IHD	Ischemic heart disease
LEHR	Low-energy high-resolution
LoA	Limits of agreement
MPS	Myocardial perfusion scintigraphy
MRI	Magnetic resonance imaging
NC	Non-attenuation correction
OSCGM	Ordered subset conjugate gradient minimizer
OSEM	Ordered subset expectation maximization
PET	Positron emission tomography
PMT	Photomultiplier tubes
SPECT	Single-photon emission computed tomography
SSS	Summed stress score

SRS	Summed rest score
SDS	Summed difference score
^{99m}Tc	Technetium-99m

Introduction

Ischemic heart disease

Ischemic heart disease (IHD) remains the leading cause of death worldwide (Khan 2020). Non-fatal IHD has a major impact on morbidity and quality of life. IHD affects around 126 million people, and the high incidence will most likely continue due to an aging population. The global cost of IHD in 2010 was around 863 billion US dollars and is expected to grow to over 1 trillion US dollars in 2030 (Khan 2020). Seeing the large impact of IHD, it is of great importance to improve disease management.

Cardiac imaging plays a vital role in diagnostic testing for suspected IHD. One such imaging method is myocardial perfusion scintigraphy (MPS). MPS is an established and widely used imaging method (Sirajuddin 2021). This thesis aims to explore quantitative aspects regarding this method.

Pathophysiology

IHD is the reduction of blood flow to the heart muscle, myocardium. This creates ischemia, an imbalance between oxygen demand and supply. This often involves coronary artery disease (CAD). CAD is the build–up of atherosclerotic plaque in the coronary arteries that supply the myocardium with blood. This is a complex process that involves inflammation and deposits of lipids. The atherosclerotic plaque can increase in size and eventually lead to a narrowing of the coronary artery that will reduce the blood flow to a point where ischemia arises. This condition is typically referred to as chronic coronary syndrome (CCS), and the plaque by then described as a stenosis (Knuuti 2020). Another possibility is that an atherosclerotic plaque ruptures. This leads to a formation of a thrombus that can give an acute occlusion of the coronary artery, typically referred to as acute coronary syndrome (ACS). It is important to point out that these are clinical presentations of CAD, but that the disease is a dynamic process that can involve different presentations in a specific patient.

In CCS the blood flow is initially maintained in affected arteries by autoregulation that involves vasodilatation (Severino 2020). If the disease progresses this regulatory system is compromised, at first only during high metabolic demands, like

physical exercise. Hence symptoms of myocardial ischemia in CCS first often manifest during such activities. Ischemia can produce symptoms like chest pain and dyspnea, but patients may also have atypical or no symptoms.

If the ischemia is severe enough the end result will be myocardial infarction, which is the irreversible tissue death of myocardium. This typically is the result of an ACS. This can lead to impaired heart function with heart failure that reduces the heart's ability to pump enough blood to support the organs with oxygen.

Diagnosis and treatment

To improve the outcome of IHD it is vital with an early and accurate diagnosis. The initial diagnostic management typically consists of multiple steps (Knuuti 2020). Firstly, one must identify patients with symptoms indicative for ACS. In patients without such symptoms the next step is to evaluate the patient's general condition and other potential causes. After basic testing and assessment of left ventricular function, diagnostic testing is considered depending on the likelihood of CAD. Diagnostic testing often includes some kind of cardiac imaging method. Once a CAD diagnosis has been confirmed, therapy is decided based on the estimated event risk. Therapy includes lifestyle management, medical therapy, and revascularization. Medical therapy aims to reduce symptoms, halt the progression of atherosclerosis, and reduce the risk of future major cardiovascular events. Revascularization also aims to reduce symptoms and reduce the risk of future major events.

Cardiac Imaging

Cardiac imaging methods have become an essential part of diagnosing and managing IHD and includes both invasive and noninvasive methods. These methods can be anatomical or functional in nature. Besides their use in diagnosing patients with suspected IHD the findings will also affect prognosis assessment and treatment. Different methods are used depending on the clinical likelihood for IHD (Saraste 2019) and availability. Since MPS is the method used in the studies included in this thesis, more emphasis will be placed on this description.

Myocardial perfusion scintigraphy

MPS is a noninvasive functional method where single-photon emission computed tomography (SPECT) is used to visualize the perfusion of the myocardium (tissue blood flow), mainly the left ventricle, and evaluate potential IHD. MPS can also assess myocardial function using electrocardiogram (ECG)-gated images. A

radiopharmaceutical is injected intravenously in the patient that will distribute in the myocardium in proportion to blood flow. Gamma radiation is emitted and captured by a gamma camera resulting in an image. MPS remains the most used noninvasive cardiac imaging method because of its availability, well-established protocols and years of data allowing for accurate diagnostic analysis and risk assessment (Sirajuddin 2021).

Radiopharmaceuticals

A radioactive tracer, or a radiopharmaceutical, is a chemical compound in which a radionuclide is coupled to a tracer substance. The properties of the tracer substance will decide the distribution of the compound in the examined system. In MPS the radioactive tracer will reside in viable myocytes, cardiac muscle cells. Today mainly two different tracers labelled with the radionuclide technetium-99m (^{99m}Tc) are used in MPS: ^{99m}Tc-2-methoxyisobutylisonitrile (sestamibi) and ^{99m}Tc-1,2-bis[bis(2-ethoxyethyl) phosphino] ethane (tetrofosmin) (Verberne 2015). These tracers are cationic complexes that are taken up by myocytes in proportion to blood flow. The uptake mechanism is not entirely known but probably depending on potential driven diffusion across membranes where the tracers to some extent also enter mitochondria (Arbab 1996, Platts 1995). Compared to the earlier used radioactive tracer, thallium-201, they have a relatively short half-life of 6 h, allowing for higher activities to be administrated, and emits higher energy gamma photons at 140 keV. This will lead to better quality images and lower radiation burden for the patient.

Stress and rest test

An MPS examination includes a stress test in connection to the radiopharmaceutical being injected in the patient. This can be done with either exercise, using a bicycle ergometer or a treadmill, or with a pharmacological stress test (Verberne 2015). In the latter either a vasodilator drug like adenosine or regadenosone is used, or a drug with positive chronotropy or inotropy, like dobutamine. The stress test results in increased blood flow in the coronary arteries either by increased myocardial oxygen demand (exercise or dobutamine) or by inducing vasodilation independent of oxygen demand (adenosine or regadenosone). The radiopharmaceutical is injected at what should be maximal vasodilatation. In blood vessels with an atherosclerotic plaque decreasing the vessel diameter, blood flow will increase less compared to healthy vessels. This is because this narrowing has led to vessels distal of the stenosis dilating already at rest to preserve normal flow, so the flow reserve at stress will be reduced. The uptake of the radiopharmaceutical by the myocardium reflects the blood flow at the time of the injection.

A rest test is also performed. However, if the stress test is considered normal, the rest study can be omitted. In the rest study, the radioactive tracer is injected at rest, without an increased blood flow in the coronary arteries. This can be done either the same day as the stress test or on a separate occasion (Verberne 2015).

Image acquisition and reconstruction

After the stress or rest test the radionuclide now resides in the heart muscle cells, the myocardium. Image acquisition is done with SPECT technology. The radionuclide decays and emits photons in the form of gamma radiation. A gamma camera is used to detect the photons and create in image (Anger 1964). In general, a gamma camera consists of a detector, a collimator and photomultiplier tubes (PMTs).

The detector is made of a scintillation crystal, typically sodium iodide. The crystal absorbs gamma photons and convert some of the energy into visible light. PMTs detect this light and convert it into electricity. A computer then constructs an image based on these signals. To be able to locate the source of the original gamma photon information about the angle of the detected photons is needed. For this, a collimator is used. The collimator sits in front of the detector and consists of material with high density and high atomic number, usually lead or tungsten, that will restrict the passage of photons. The collimator is pierced with holes and allows photons with a certain angle to pass through. Traditionally, the most used collimator type for MPS has been parallel hole collimators, and this collimator type is still used as standard in clinical practice (Dorbala 2018). This collimator consists of a lead plate where all the holes are parallel to each other, see figure 1. This will only allow for photons travelling perpendicular to the holes to reach the detector. The resolution and sensitivity will depend on the size of the holes. Large diameter holes will increase sensitivity but decrease resolution. Different types of parallel hole collimators are named after sensitivity, resolution, and energy. Thicker wall between the holes (septa) will be used in higher energy collimators. In recent years new technique has made more complex collimator design possible (Van Audenhaege 2015). Some of these new collimators are part of complete cardiac-centered gamma camera systems. This allows for decreased radiopharmaceutical activity, reducing the radiation exposure to patients, or a shorter acquisition time. One such system is the IQ-SPECT system (Siemens Healthineers, Erlangen, Germany), that increases the sensitivity, collecting up to 4 times more counts compared to systems with parallel hole collimators (Hyafil 2019). This system uses a multifocal collimator with convergent symmetry around the center, called SMARTZOOM, see figure 1. Further out close to the edge of the collimator the holes are almost parallel, to reduce truncation. The IQ-SPECT orbit is centered on the heart keeping it in the collimator's magnification area.

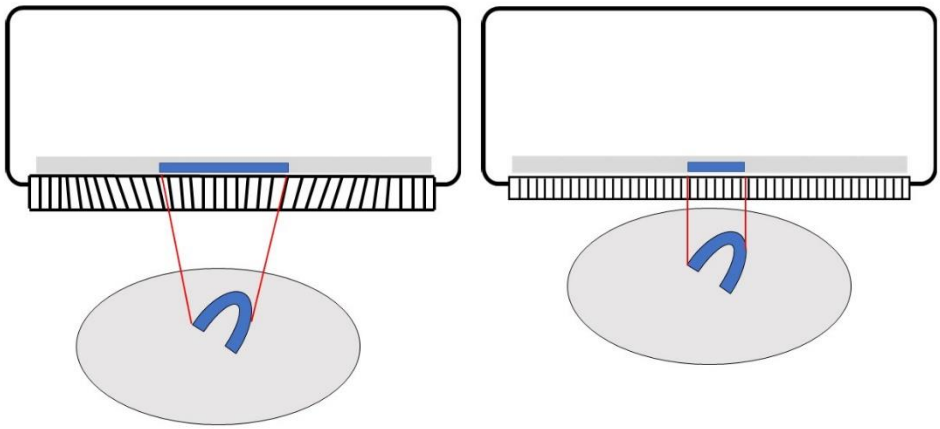

Figure 1. The left part of the image shows a multifocal collimator, and the right side shows a conventional parallel hole collimator.

A gamma camera can produce planar images in two dimensions, with a computer creating a matrix of pixels corresponding to the signals from the detector. When planar images are acquired, no information about depth is obtained, and signals from separate structures can overlap. With SPECT technology, tomographic three-dimensional images can be created. This is achieved by letting the detectors rotate around the patient and acquire projections from multiple angles. Image reconstruction based on these projections can then be performed. Two different methods of reconstruction are available: filtered back projection (FBP) and iterative reconstruction (Ravishankar 2020). The concept of FBP is to first filter the data from all the projections and then run them back through the image to obtain an approximation of the original. Each projection row corresponds to the sum of all signals from that specific line through the object. Since the projections are limited in number, they need to be filtered to reduce artefacts and blurring of the image. The other method for image reconstruction, iterative reconstruction, starts with an estimation of the image, typically this estimation is uniform intensity. Projection data is estimated using forward projection which is then compared to measured projections. This comparison is back projected and used to update the image estimation. This process is then repeated until estimated projections agree with the measured projections. A common iterative reconstruction method is the ordered subset expectation maximization (OSEM) method.

An important aspect of image reconstruction is attenuation correction (Patton 2008). Attenuation is the loss of energy of a photon traversing matter. The main mechanism for this in SPECT is Compton scattering, where a photon interacts with an electron

and scatter, losing some of its energy. This can lead to both loss of information, if photons that were on a trajectory to pass the collimator now misses it, and to false signals if scattered photons are detected. To combat this issue X-ray computed tomography (CT) can be used in conjunction with SPECT (Hutton 2014). Information from the CT images are used to create a density map which is used for attenuation correction in the SPECT images. A density map used for attenuation correction can also be obtained by rotating a Gadolinium source around the patient. If attenuation correction is unavailable, images can be acquired with the patient in prone position, in addition to the standard supine position. This does not eliminate attenuation artefacts, but they will change location, while true defects will remain unchanged (Hahn 2021).

Gated SPECT can be used to obtain information about cardiac function in addition to assessment of coronary blood flow (Mansoor 1999). Gated image acquisition is guided by ECG. The acquisition starts with the R wave on ECG, corresponding to end-diastole. The cardiac cycle is then divided in multiple frames (often 8 or 16 frames) and data from each frame is added up over many cycles (Paul 2004). This will generate a volume curve, representing the left ventricle volume for each of the frames. End-diastolic volume (EDV) and end-systolic volume (ESV) for the left ventricle are obtained as well as left ventricular ejection fraction (EF). From these gated images, regional wall motion can also be estimated (Verberne 2015).

Interpretation

The generated images are then processed using computer software. The left ventricle is segmented and often presented in one short axis view and two long axis views (vertical and horizontal). The short axis view is displayed with slices going from the base to the apex of the left ventricle. The two long axis views are displayed with slices going from the septum to the lateral wall, and from the inferior wall to the anterior wall, respectively, see figures 2 and 3. Besides these three views a polar plot is usually also created for interpretation purposes, see figure 2. This plot displays left ventricular perfusion in a single two-dimensional image, facilitating interpretation comparing different regions of the left ventricle in the same image. In this plot the apex is in the center and the basal parts on the outer edge. The polar plot is typically divided into 17 segments (Czaja 2017). The polar plot can be also divided into territories corresponding to the coronary vessels, see figure 2. Typically, the intensity of the signal is set to maximum in the region with the highest signal and the rest of the image is normalized in relation to this maximum.

Interpretation of reconstructed images is done in dedicated, commercially approved, MPS software (Dorbala 2018). Different types of color scales or grayscales can usually be applied. After evaluation of potential artifacts and image quality, the images are analyzed regarding myocardial perfusion, reflected by tracer distribution, and left ventricular function, if ECG-gated images were obtained. The

examination will either consist of both stress and rest images or only stress images. If attenuation correction has been applied these images will be visualized as well.

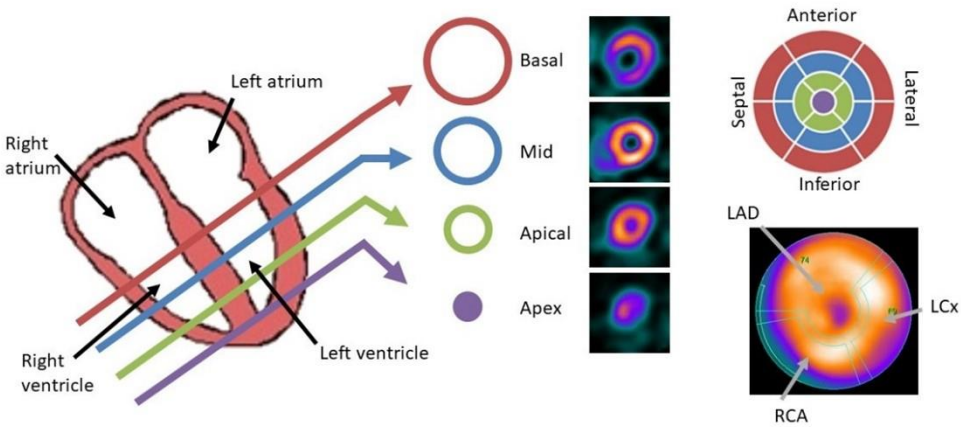

Figure 2. How the short axis views of the left ventricle are obtained, from the basal part to the apex. The upper right image shows a polar plot with the 17-segment model. The lower right image shows a polar plot where the typical territories for the different coronary arteries are shown. LAD = left anterior descending artery. LCx = left circumflex artery. RCA = right coronary artery.

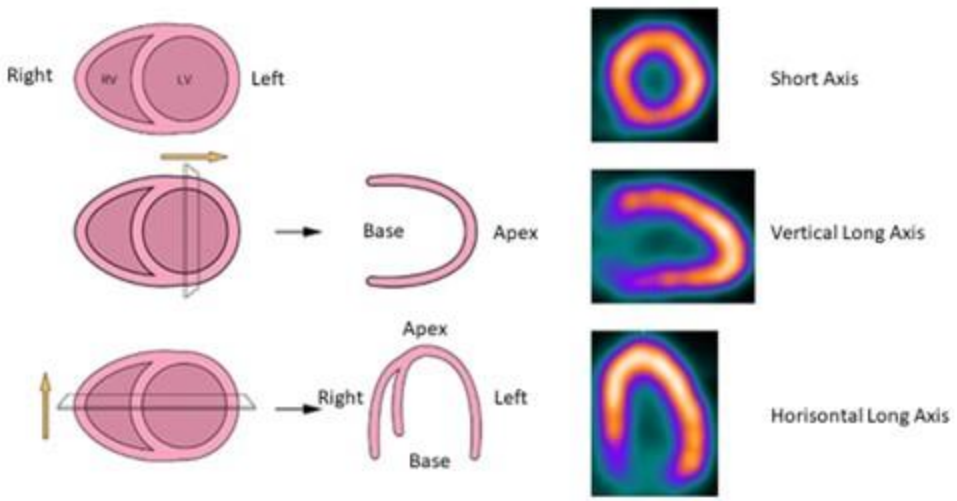

Figure 3. Short and long axis views of the left ventricle.

If the patient only underwent a stress examination this usually indicates the images were assessed as normal, with uniform perfusion and normal function with no indications for IHD. If the patient underwent both stress and rest examinations, these images are compared regarding myocardial perfusion and function. If uniform perfusion and normal function is seen in both rest and stress images the examination is assessed as normal. If perfusion defects of the same size and localization is present in both rest and stress this usually indicates a myocardial infarction (or potentially hibernating myocardium). If perfusion defects are found in stress images that are not present in rest images this indicates stress-induced ischemia. Stress-induced ischemia can also be suspected with significantly reduced function in gated stress-images compared to rest.

Myocardial perfusion defects are evaluated in the reconstructed slices and the polar plot using visual and qualitative analysis. The three image views (short axis and two long axis) will be visualized and inspected, preferably simultaneously, see figure 4. In addition, semi quantitative analysis is also recommended (Dorbala 2018). Using the 17-segment model for the polar plot, defect severity is scored from 0 to 4, with 0 being normal perfusion and 4 being no perfusion (with normal perfusion being derived from a reference population). The number of segments with reduced perfusion will correspond to defect extent. A global estimation of perfusion is obtained by combining severity and extent for all 17 segments into a single measure, summed stress score (SSS) for the stress examination and summed rest score (SRS) for the rest examination. Summed difference score (SDS) can then be calculated by subtracting SRS from SSS, being the degree of reversible perfusion defect, and potentially ischemia. Percent of affected myocardium, SS%, can be calculated with dividing SSS with the maximum value (being 68 in a 17-segment model) and multiplying with 100 (Czaja 2017). Quantitative analysis can also be made, comparing regional tracer uptake with a reference population, expressed as standard deviation.

Finally, the procedure and interpretation of the study is described in a written report, sent to the referring, or treating physician (Trägårdh 2015).

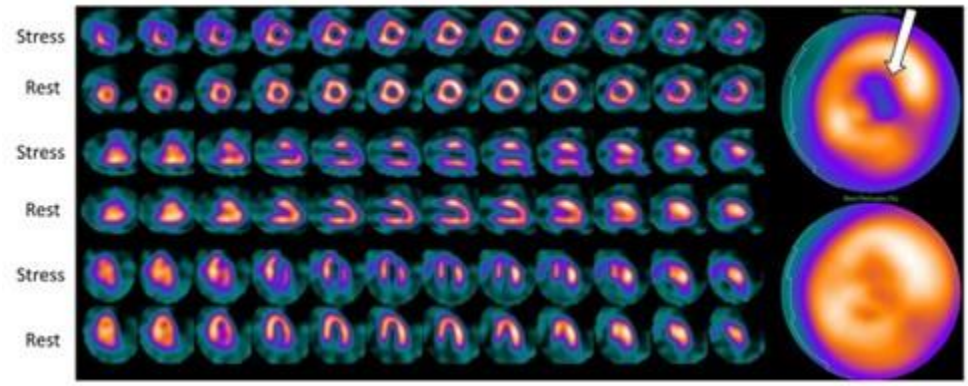

Figure 4. Short axis, vertical long axis, and horizontal long axis images. Polar plot images are shown to the right. This patient has reduced perfusion during stress in apical/anterior parts of the left ventricle (arrow in the upper right image), but normal perfusion at rest (lower right image). This indicates stress-induced ischemia.

Other cardiac imaging methods

Invasive coronary angiography

Invasive coronary angiography is considered the standard diagnostic imaging method for patients with suspected CAD (Sirajuddin 2021). Iodine-based contrast agent is used in conjunction with X-rays to evaluate the blood flow in the coronary arteries. Fractional flow reserve (FFR) can be used to calculate the pressure ratio before and after a plaque and with that estimate the degree of stenosis. The main benefit with coronary angiography is that besides the diagnostic possibilities, intervention can be performed at the same time with percutaneous coronary intervention. But since the method is invasive it involves some risk and many times a non-invasive method is preferred initially.

Computed tomography angiography

Coronary computed tomography angiography (CCTA) is a non-invasive anatomical method used to visualize the coronary arteries with iodine-based contrast and X-rays. CCTA will identify atherosclerotic plaque and estimate the degree of stenosis. The main benefit of this method is its negative predictive value of 99%, where a negative test in most cases excludes CAD (Sirajuddin 2021).

Magnetic resonance imaging

Cardiac magnetic resonance imaging (cardiac MRI) is a non-invasive method used for both anatomical and functional assessments of the heart (Pahlm 2011). A powerful magnetic field and radio waves are used together with the natural magnetic properties of hydrogen atoms in the body to generate images. An extracellular contrast agent, Gadolinium, is often used. Cardiac MRI is considered the gold

standard for evaluating heart volumes and function, as well as myocardial infarction (Salerno 2017). Cardiac MRI can also be used to assess myocardial perfusion. This is done with using a vasodilatory substance and assessing first pass perfusion of Gadolinium.

Positron emission tomography

Positron emission tomography (PET) is a non-invasive method that is similar to MPS as it also detects radiation emitted from a radionuclide coupled to a tracer substance (Sirajuddin 2021). PET uses positron emission, where the positron will collide with an electron, and annihilation resulting in two gamma photons that can be detected. PET has better resolution compared to MPS and can also be used for quantitative measurements of perfusion. PET is considered the gold standard for quantification of myocardial perfusion. Depending on the radiopharmaceutical used, either cardiac perfusion or viability can be assessed.

Echocardiography

Echocardiography uses ultrasound to create images of the heart. It is a readily available non-invasive method used for assessing cardiac anatomy and function. Stress echocardiography can be used on patients with suspected CAD. Regional wall motion is assessed in rest and stress (exercise or pharmacological), with reduced motion in stress indicating ischemia. The main disadvantage is that suboptimal image quality sometimes can limit the ability to diagnose disease (Pahlm 2011).

Aims

The general aim of this thesis is to gain knowledge about different quantitative aspects on MPS – from developing a new method that could potentially aid in the visual interpretation of images to comparing images obtained from different SPECT cameras.

The specific aim for each paper was to:

I. Test the concept of the perfusion vector in simulated MPS images and then to validate the method in a clinical setting.

II. Compare the IQ-SPECT and its multifocal collimator with a conventional SPECT camera with parallel hole collimator regarding stress perfusion data, left ventricular EF and cardiac volumes.

Materials and methods

Study population

In the first study 1283 patients who underwent a MPS examination, both stress and rest, in a clinical setting during 2007 in Malmö, Sweden, were considered for inclusion. The patients were categorized into groups depending on the visual interpretation of the examination. The first ten in each group assessed with having specific perfusion defects were included. The specific defects were located in the anterior, apical, lateral, or inferior left ventricle wall, either assessed as stress-induced ischemia or as infarction. For the group assessed with having normal myocardial perfusion the first 40 were included. In total 120 patients were included.

In the second study 41 patients who were referred for a MPS and agreed to be examined on both camera systems were included, regardless of the examinations being assessed as normal or as having perfusion defects. Patients were consecutively included after installation of the IQ-SPECT system in 2015. If the stress examination were assessed as having reduced perfusion these patients also underwent a rest examination. However, the number of patients with a rest study were too low for these studies to be included.

MPS protocol and image acquisition

In the first study a 2-day gated stress/non-gated rest protocol with ^{99m}Tc-tetrofosmin (600 MBq at stress and at rest) was used. The stress tests were conducted with maximal exercise on a bicycle ergometer (with patients reaching at least 85 % of predicted maximal heart rate) or with adenosine according to standard protocols. Image acquisition began 60 minutes later. Images were acquired with patients in supine position using a Siemens e.cam dual-head gamma camera (Siemens Healthineers, Erlangen, Germany), with a low-energy high-resolution (LEHR) parallel hole collimator. SPECT was used over 180° elliptical and auto-contour rotations from the 45 ° right anterior oblique position. 64 projections were obtained in a 128 x 128 matrix with an acquisition time of 25 seconds for every projection. FBP was used for image reconstruction. Tomographic reconstruction was performed on e.soft software (Siemens AG Medical Solutions, Erlangen, Germany),

generating short- and long-axis slices. No attenuation correction was applied. EXINI Heart™ (EXINI Diagnostics AB, Lund, Sweden) software was used to automatically derive the size of the perfusion defects, using an appropriate normal database.

In the second study the stress tests were performed as in study I, with the same radiopharmaceutical and dose being administered. The patients were examined in supine position with both a Siemens e.cam dual-head gamma camera and a Siemens Symbia system with IQ-SPECT (Siemens Healthineers, Erlangen, Germany). ECG-gated images were also obtained.

The Siemens e.cam was the same system as in study I, with the same LEHR parallel hole collimator and FBP used for image reconstruction of images without attenuation correction. In contrast to study I attenuation correction was applied, with a rotating Gadolinium source, ^{153}Gd multiple-line source (Siemens AG Medical Solutions, Erlangen, Germany), generating a density map. Images with attenuation correction were reconstructed using an iterative filtered back projection (6 iterations).

The Siemens Symbia system with IQ-SPECT used a multifocal collimator with SMARTZOOM. SPECT was used over 180°, starting from the 59° right anterior oblique position with a 76-degree angle between the detectors with a total of 32 angles. A 128 x 128 matrix was used with 14 seconds of acquisition time per angle. Attenuation correction was applied, using CT to create a density map. Iterative image reconstruction was used, ordered subset conjugate gradient minimizer (OSCGM), which is similar to OSEM (Onoguchi 2016). 3 iterations and 10 subsets were used for images with and without attenuation correction, while 2 iterations and 10 subsets were used for gated images.

Reconstructed images were processed and analyzed in EXINI Heart™ using the 17-segment model to automatically calculate SSS, for both images with and without attenuation correction, see figure 5. Appropriate normal databases were used. Calculations of cardiac volumes, EDV and ESV, as well as function (EF) were also automatically calculated from gated images using EXINI Heart™.

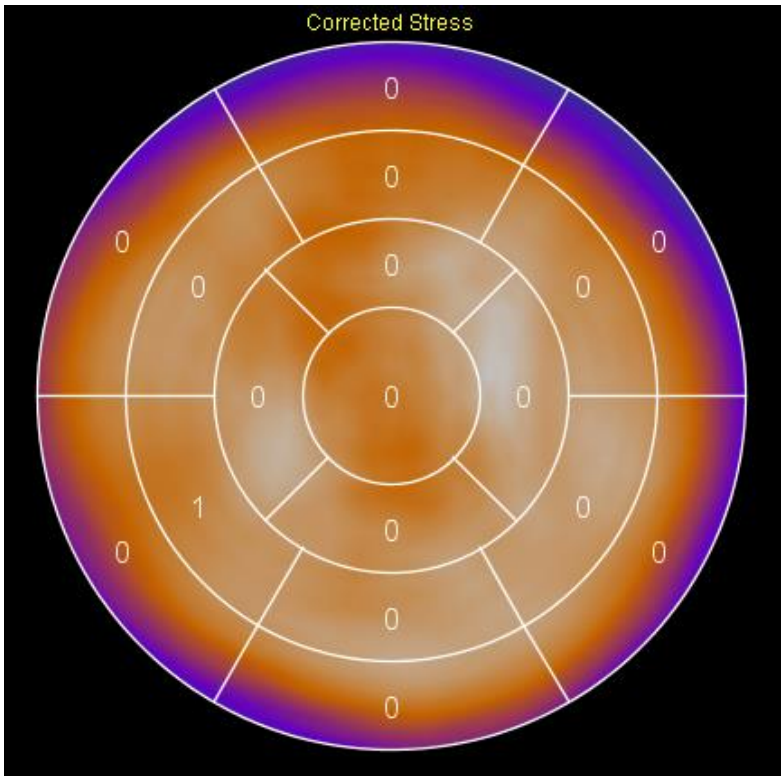

Figure 5. Polar plot with the 17 segments used to automatically calculate SSS. Attenuation correction has been applied in this image. Image from EXINI Heart™.

The concept of the perfusion vector

In the first study we introduced the concept of the perfusion vector as a quantitative method for interpretation of MPS. A vector is an object that has both a magnitude and a direction. The concept is based on the difference between the anatomical centroid and the perfusion center of gravity. The anatomical centroid being the center of gravity in a two- or three-dimensional figure, in this case the left ventricle. The perfusion center of gravity will depend on the relative perfusion in the left ventricle. If normal and close to homogenous perfusion, the location of the perfusion center of gravity will be in the proximity of the anatomical centroid. The left ventricle is outlined from MPS images using the EXINI Heart™ software and is represented by a surface of rectangles through the center of the myocardium, see figure 6. Each rectangle is assigned an index i in the grid, a center position (x, y, z), an area A, and a weight W. With $W = 1$ for all i, the anatomical centroid, C_A is calculated, see equation 1. The perfusion center of gravity, C_P, is calculated by

setting W to the measured intensity in the MPS image. The perfusion vector, $\vec{P}$, is the difference between the anatomical centroid and the perfusion center of gravity: $\vec{P} = C_P - C_A$, see figure 6. The perfusion vector would point away from the perfusion defect, this since the perfusion center of gravity will be located on the opposite side, with the magnitude corresponding to the extent of the defect and the direction expressed on the *x*-, *y*- and *z*-axes.

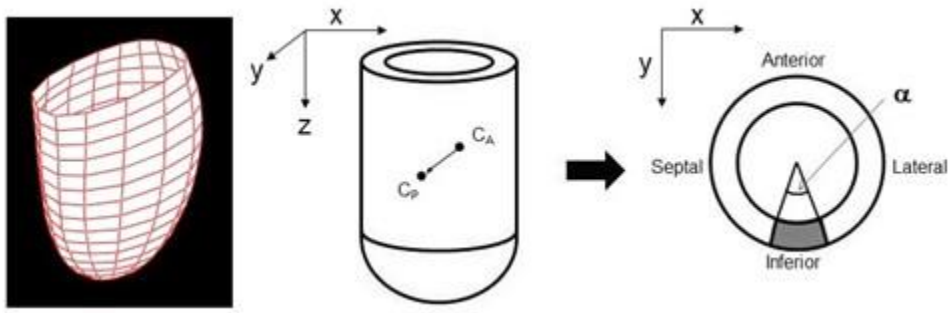

Figure 6. To the left the left ventricle as a surface of rectangles. In the middle the perfusion vector as the difference between the anatomical centroid, C_A and the perfusion center of gravity, C_P. To the right the angle, α, for a simulated defect.

$$C = \left(\frac{\sum x_i A_i W_i}{\sum A_i W_i}, \frac{\sum y_i A_i W_i}{\sum A_i W_i}, \frac{\sum z_i A_i W_i}{\sum A_i W_i} \right) \qquad (1)$$

Computer simulations

In the first study simulated MPS images were used to test the concept of the perfusion vector. Projection data was simulated with the SIMIND Monte Carlo program (Ljungberg 1989), a program that describes a standard SPECT camera. XCAT phantom (Segars 2010) was used to create a phantom of the left ventricle. The phantom was made to represent a standard male with an EDV of 148 ml. Forty static phantoms were created with the heart in different positions to simulate a beating heart and breathing motion. Eight different perfusion defects, four anterior

and four lateral defects, were simulated, with different angles, α, of 10°, 30°, 50°, and 70°, see figures 6 and 7. Simulations without perfusion defects were also performed. Iterative reconstruction was used for image reconstruction.

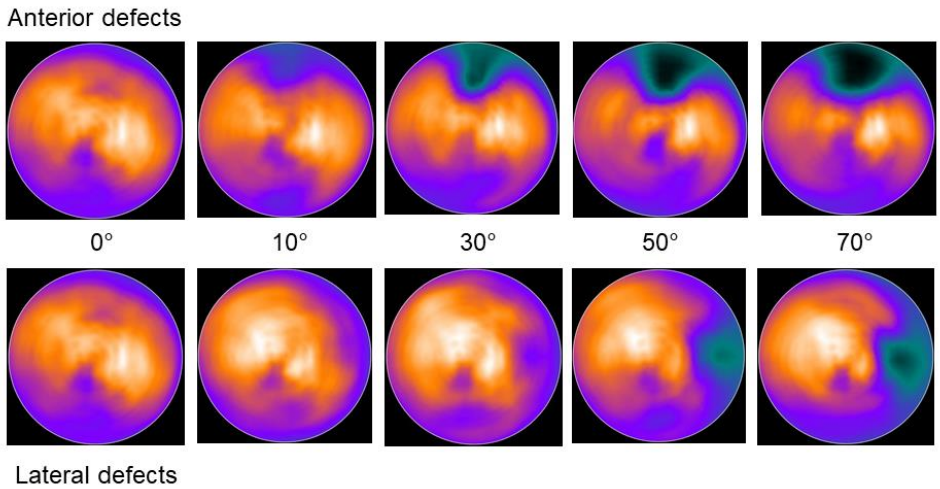

Figure 7. The upper part with simulated anterior defects and the lower part with simulated lateral defects. The first image in both rows without a defect.

Statistical analysis

In study I Kruskal-Wallis analysis were performed to investigate for differences between normal and abnormal perfusion. When this was found, Mann-Whitney's test was used to test for differences. Patients with perfusion defects were compared to the patients with normal perfusion. Since multiple comparisons were performed, a Bonferroni correction was applied and a significance level of 0.0125 was used when four groups were tested and 0.025 when two groups were tested. Spearman's correlation test was done to investigate the correlation between defect extent and vector magnitude.

In study II Bland-Altman analysis was performed to test for bias and limits of agreements when comparing the two different camera systems.

Results and discussion

Perfusion vector in simulated and patient MPS images

Interpretation of MPS examinations still largely relies on visual assessments that is known to have inter- and intra-observer variability. The aim of the first study was to test the concept of the perfusion vector as an objective quantitative method for assisting in the interpretation of MPS images. Both simulated MPS images and MPS images from selected patient examinations were analyzed.

A perfusion vector was calculated, $\vec{P} = C_P - C_A$, for all simulated perfusion defects. For anterior defects, the stress perfusion vector on the *y*-axis (anterior-inferior direction) increased according to defect size, while it remained stable on the other axes, see figure 8. For lateral defects, the stress perfusion vector on the *x*-axis (septal-lateral direction) decreased according to defect size, while it remained more stable on the other axes, see figure 8.

For anterior defects the stress perfusion vector should increase on the *y*-axis, since this axis is in anterior-inferior direction, see figure 6, and the vector points away from the defect. For lateral defects the stress perfusion vector should decrease on the *x*-axis since this axis is in septal-lateral direction and the vector would then point in septal direction. Hence, the stress perfusion vector behaved as expected.

Seeing the concept work in simulated MPS images, the same method was then applied to patient MPS images. Mean total defect extent (automatically derived from EXINI Heart^{TM}) was 0.17 % for the normal group and 25 % for the abnormal group, patients assessed with having perfusion defects (15.6 % for ischemic defects and 29.8 % for infarction). Stress perfusion vectors were calculated and compared between the normal group and four different abnormal groups assessed with having apical, inferior, anterior, or lateral perfusion defects. No distinction between ischemia and infarction were done.

An important finding was that the perfusion vector range was small in all three orientations for the normal group, indicating a low inter-individual variability, while larger ranges was seen in the abnormal group, see figure 9. This means it could be possible to use this method to help determine if a stress examination is normal, hence reducing the amount of rest examinations that needs to be performed.

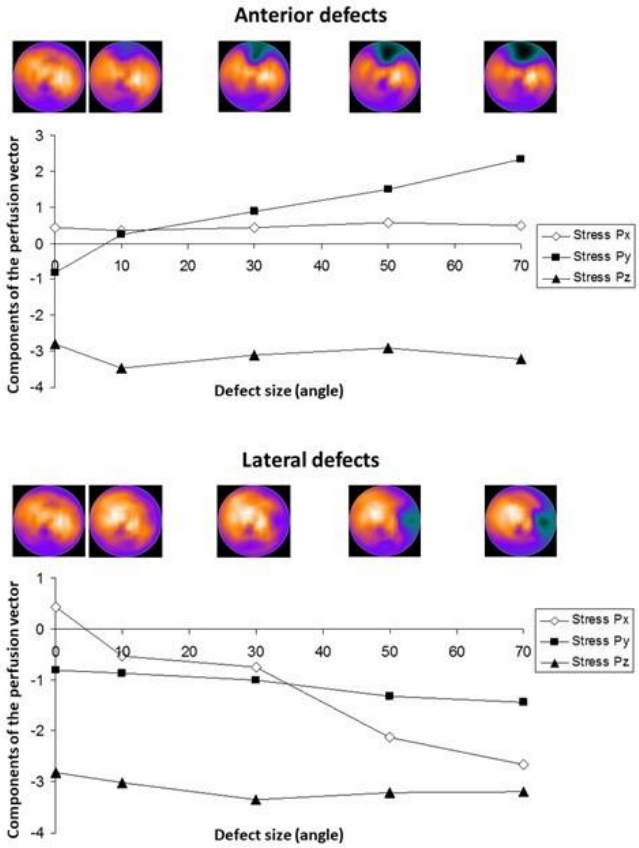

Figure 8. Simulated MPS images. The upper image showing the perfusion vector for anterior defects and the lower image the perfusion vector for lateral defects.

Significant differences were found on all axes when comparing the normal group to the groups with apical or lateral defects, see figure 9. For inferior defects only the *y*-axis was significantly different and for the anterior defects the same was true for the *z*-axis (and not on the *y*-axis as expected). Seeing apical defects affecting the perfusion vector in the opposite direction compared to lateral defects on the *x*-axis and in the opposite direction compared to inferior defects on the *y*-axis can be explained with apical defects often being located more towards the septal and anterior part of the left ventricle. Lateral defects changed the perfusion vector drastically on the *x*-axis, as expected. Lateral defects also changing the perfusion vector on the *y*-axis can be explained with these defects often being located slightly inferior in the left ventricle. Changes on the *z*-axis will depend on where the defect is located in the apical-basal direction in the left ventricle. Apical defects were included as a separate group to examine if such changes existed, and as expected the perfusion vector for apical defects changed drastically on this axis.

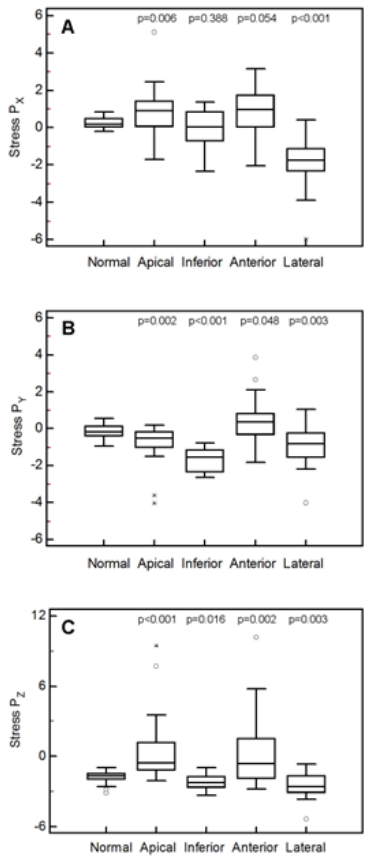

Figure 9. Box plots for stress perfusion vectors for normal patients and for patients with perfusion defects (ischemia or infarction) in different locations for the x-axis (A), y-axis (B) and z-axis (C). The p-value is related to the normal group.

There was a significant correlation between defect size and stress vector magnitude (vector size) with the magnitude increasing with larger defect extent ($r = 0.63$, $p < 0.001$). When comparing the difference vector magnitude (the difference between stress and rest vector magnitude), there was a significant difference between normal patients and patients with defects assessed as ischemia, but not with patients assessed as having infarction, see figure 10. This could potentially be used to distinguish between normal patients and patients with ischemia, but a large inter-individual variability was also found. This variability could possibly be explained with the patients in the abnormal group being selected only for the localization of the perfusion defect, not the size. Another possible reason is the fact that patients will not have completely homogenous perfusion in areas not assessed as having significant perfusion defects, which will affect the calculation of the perfusion vector.

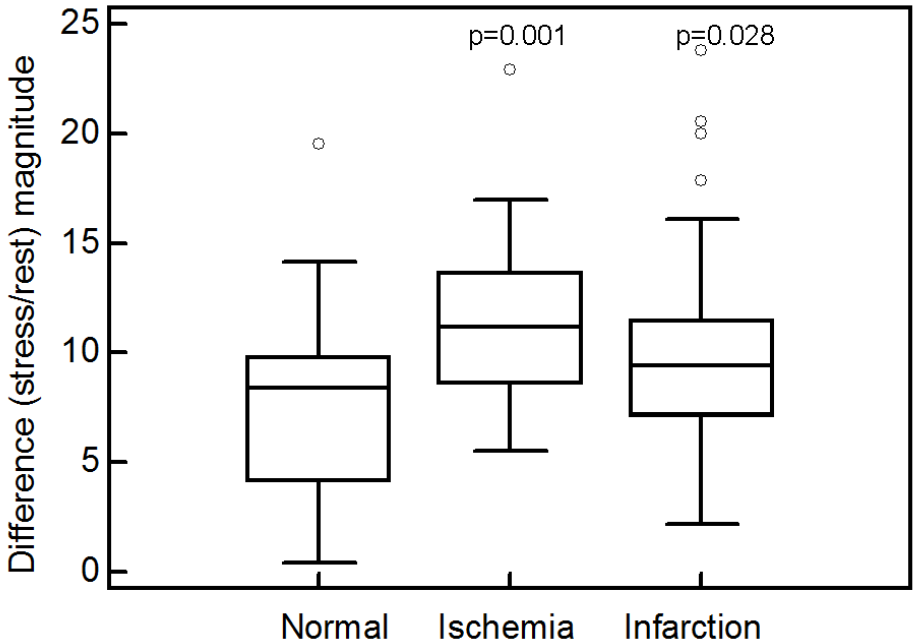

Figure 10. Box plots for the difference magnitude for normal patients and for patients with ischemia and infarction. The p-value is related to the normal group.

Quantitative data comparing two MPS SPECT systems

This study aimed to compare IQ-SPECT with conventional gamma cameras regarding both stress perfusion data (SSS) and left ventricular volumes (EDV and ESV) and function (EF). This to investigate for differences affecting interpretation of MPS examinations. Previous patient studies (Leva 2020, Havel 2014) and phantom studies (Hippeläinen 2017) comparing the new IQ-SPECT gamma camera system with its multifocal collimator with conventional gamma cameras with parallel hole collimators have shown somewhat conflicting results and some studies only investigate left ventricular volumes and function and not perfusion data.

For stress perfusion data, SSS, similar mean values were found, both for images with attenuation correction (AC) and with no attenuation correction (NC), see table 1. Left ventricular volumes (EDV and ESV) were lower for the IQ-SPECT system whereas left ventricular EF were higher for the IQ-SPECT system.

Table 1. Quantitative parameters in IQ-SPECT and conventional SPECT

Parameter (mean±SD)	IQ-SPECT	Conventional SPECT
SSSAC	9.9±7.8	11.2±8.1
SSSNC	8.8±8.2	10.6±9.1
EDV (ml)	87.3±32.0	104.1±31.3
ESV (ml)	19.9±20.3	29.3±19.4
EF (%)	81.1±14.0	74.0±11.4

Bland-Altman analysis were used to analyze the agreement between the two methods, see figure 11. A low bias was found for SSS. Bias was larger for cardiac volumes and EF. Limits of agreement (LoA) were overall large, especially for EF.

The findings indicate that there should be no majorly different approach, on a group level, to assess stress perfusion when using the IQ-SPECT system compared to conventional SPECT. The EXINI Heart™ software was used to automatically generate SSS using the 17-segment model. At our department we normally use these numbers together with visual assessment to evaluate perfusion. There is no real consensus on the best method and some departments more heavily emphasize automated analysis.

MPS is known to underestimate left ventricle volumes (Hedeer 2010). The findings in this study indicate that IQ-SPECT might underestimate volumes even more than conventional SPECT. EF was found to be higher with IQ-SPECT, a parameter that also has been shown to vary in previous studies.

A reason for these variations in findings could be that different studies used different reconstruction parameters for the MPS images. This can influence the measurements of cardiac volumes and function. Further studies comparing the influence of different reconstruction parameters on left ventricular volumes and function should be performed in order to optimize the method. Cardiac MRI could be used as a reference method.

Studies also used different software to automatically calculate SSS, volumes and function, which have been shown to affect these measurements (Ather 2014). Also, it is not always clear what normal databases were used in different studies.

The European Association of Nuclear Medicine has now published guidelines for MPS using cardiac-centered gamma cameras, such as the IQ-SPECT system (Hyafil 2019). Here, recommendations regarding image acquisition and interpretation are provided.

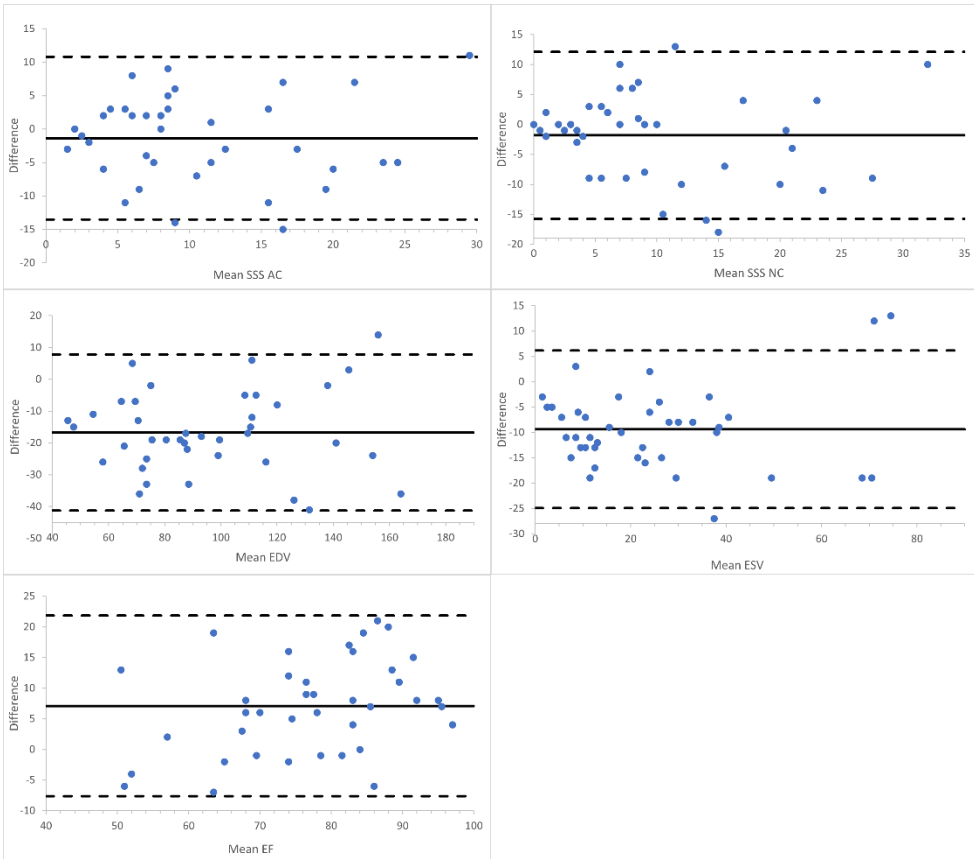

Figure 11. Bland-Altman analysis for agreement between IQ-SPECT and conventional SPECT for SSS (with and without attenuation correction), EDV, ESV and EF. Solid lines indicate bias and dashed lines indicate the 95% LoA. Difference on the y-axis is IQ-SPECT - conventional SPECT.

Ethical considerations

Ethical permissions from the local research committee at Lund University were obtained for both studies. For study I, only clinical examinations were performed and only some basic information from the medical records were needed. For study II an additional image acquisition was needed, but only patients that were fit enough for this were asked to be included. A low-dose CT for attenuation correction was needed for the examinations with the IQ-SPECT system giving the patients

additional radiation exposure. However, since most patients referred to a MPS are over 50 years old, the additional risk was regarded as negligible.

Limitations

For both studies only a relatively small number of patients were included, and no other methods were used to validate the interpretation of the MPS images. In study I there was no true normal control group since all the included patients were referred to a clinical MPS. In study II data from rest examinations were not included since most patients only did a stress examination. The software EXINI Heart™ is no longer registered for clinical use in Europe.

Conclusions

I. The perfusion vector was shown to have potential in assisting the visual interpretation of MPS examinations. The small variation in vector magnitude in normal patients compared to patients with perfusion defects could be used to decide if a stress study is normal or not, and possibly reduce the amount of rest studies needed to be performed. Further studies are needed to validate the concept.

II. No major differences in the interpretation of MPS studies regarding perfusion data can be expected between the IQ-SPECT system and a conventional SPECT system. However, cardiac volumes were lower and EF higher for IQ-SPECT examinations, which should be further investigated using a reference method.

Populärvetenskaplig sammanfattning

Ischemisk hjärtsjukdom är en allvarlig folksjukdom. Den orsakas av förträngningar i de kärl, kranskärlen, som försörjer hjärtat med blod. Detta kan ge upphov till syrebrist i hjärtmuskeln vilket försämrar hjärtats funktion. Om denna syrebrist blir uttalad kan delar av hjärtmuskeln dö, vilket kallas för hjärtinfarkt.

Olika metoder används för att diagnostisera ischemisk hjärtsjukdom. En av dessa metoder är myokardscintigrafi. Här används ett radioaktivt ämne som binder in till hjärtmuskeln beroende på hur bra kranskärlen fungerar. Sedan fångar en kamera upp den strålning som hjärtat avger när det radioaktiva ämnet sönderfaller. På bilderna kan man sedan se om det finns tecken på syrebrist i hjärtmuskeln och även bedöma hjärtats storlek och funktion.

Denna studie avser att undersöka och möjligen förbättra hur man kan bedöma dessa bilder från myokardscintigrafi. I den första studien beräknas en så kallad *vektor*, vilket är en matematisk storhet som har både storlek och riktning, för olika bilder från myokardscintigrafi. En vektor kan liknas med en pil som har en viss riktning och längd. Det visade sig att denna vektor förändrades beroende på hur hjärtats blodförsörjning såg ut. Denna metod skulle kunna vara till hjälp när man bedömer bilder från myokardscintigrafi. I den andra studien jämförs ett nyare kamerasystem med det som använts tidigare. Det nya systemet har teknik som möjliggör bättre upplösning och lägre stråldos eller kortare tid i kameran. Det visade sig att bedömningen av hjärtats blodförsörjning inte skilde sig så mycket åt. Däremot skiljde sig bedömningen av hjärtats storlek och funktion. Detta är kunskap som kan vara till hjälp när man ska bedöma bilder från myokardscintigrafi.

Acknowledgements

I would like to thank:

Elin Trägårdh, my supervisor, for always being there with encouragement and great patience.

Per Wollmer, my co-supervisor and ST-supervisor, for his wisdom.

Lars Edenbrandt, my co-supervisor, for his guidance.

David Minarik, author, and co-author, for explanations of many of the technical aspects regarding nuclear medicine.

All the co-authors.

All my colleagues at Clinical Physiology and Nuclear medicine.

References

Anger HO. Scintillation Camera with multichannel collimators. J Nucl Med. 1964 Jul;5:515-31.

Arbab AS, Koizumi K, Toyama K, Araki T. Uptake of technetium-99m-tetrofosmin, technetium-99m-MIBI and thallium-201 in tumor cell lines. J Nucl Med. 1996 Sep;37(9):1551-6.

Ather S, Iqbal F, Gulotta J, Aljaroudi W, Heo J, Iskandrian AE, Hage FG. Comparison of three commercially available softwares for measuring left ventricular perfusion and function by gated SPECT myocardial perfusion imaging. J Nucl Cardiol. 2014 Aug;21(4):673-81.

Czaja M, Wygoda Z, Duszańska A, Szczerba D, Głowacki J, Gąsior M, Wasilewski JP. Interpreting myocardial perfusion scintigraphy using single-photon emission computed tomography. Part 1. Kardiochir Torakochirurgia Pol. 2017 Sep;14(3):192-199.

Dorbala S, Ananthasubramaniam K, Armstrong IS, Chareonthaitawee P, DePuey EG, Einstein AJ, Gropler RJ, Holly TA, Mahmarian JJ, Park MA, Polk DM, Russell R 3rd, Slomka PJ, Thompson RC, Wells RG. Single Photon Emission Computed Tomography (SPECT) Myocardial Perfusion Imaging Guidelines: Instrumentation, Acquisition, Processing, and Interpretation. J Nucl Cardiol. 2018 Oct;25(5):1784-1846.

Hahn E, Kammieier A, Burchert W, Lindner O. Attenuation correction in CZT myocardial perfusion imaging comparison of supine-prone and low-dose CT-corrected supine acquisitions. Nucl Med Commun 2021 Aug 1;42(8):884-891.

Havel M, Kolacek M, Kaminek M, Dedek V, Kraft O, Sirucek P. Myocardial perfusion imaging parameters: IQ-SPECT and conventional SPET system comparison. Hell J Nucl Med. 2014 Sep-Dec;17(3):200-3.

Hedeer F, Palmer J, Arheden H, Ugander M. Gated myocardial perfusion SPECT underestimates left ventricular volumes and shows high variability compared to cardiac magnetic resonance imaging -- a comparison of four different commercial automated software packages. BMC Med Imaging. 2010 May 25;10:10.

Hippeläinen E, Mäkelä T, Kaasalainen T, Kaleva E. Ejection fraction in myocardial perfusion imaging assessed with a dynamic phantom: comparison between IQ-SPECT and LEHR. EJNMMI Phys. 2017 Dec;4(1):20.

Hutton BF. The origins of SPECT and SPECT/CT. Eur J Nucl Med Mol Imaging. 2014 May;41 Suppl 1:S3-16.

Hyafil F, Gimelli A, Slart RHJA, Georgoulias P, Rischpler C, Lubberink M, Sciagra R, Bucerius J, Agostini D, Verberne HJ; Cardiovascular Committee of the European Association of Nuclear Medicine (EANM). EANM procedural guidelines for myocardial perfusion scintigraphy using cardiac-centered gamma cameras. Eur J Hybrid Imaging. 2019 Jul 2;3(1):11.

Patton JA, Turkington TG. SPECT/CT Physical Principles and Attenuation Correction. Journal of Nuclear Medicine Technology Mar 2008, 36 (1) 1-10

Khan MA, Hashim MJ, Mustafa H, Baniyas MY, Al Suwaidi SKBM, AlKatheeri R, Alblooshi FMK, Almatrooshi MEAH, Alzaabi MEH, Al Darmaki RS, Lootah SNAH. Global Epidemiology of Ischemic Heart Disease: Results from the Global Burden of Disease Study. Cureus. 2020 Jul 23;12(7):e9349

Knuuti J, Wijns W, Saraste A, Capodanno D, Barbato E, Funck-Brentano C, Prescott E, Storey RF, Deaton C, Cuisset T, Agewall S, Dickstein K, Edvardsen T, Escaned J, Gersh BJ, Svitil P, Gilard M, Hasdai D, Hatala R, Mahfoud F, Masip J, Muneretto C, Valgimigli M, Achenbach S, Bax JJ; ESC Scientific Document Group. 2019 ESC Guidelines for the diagnosis and management of chronic coronary syndromes. Eur Heart J. 2020 Jan 14;41(3):407-477.

Leva L, Matheoud R, Sacchetti G, Carriero A, Brambilla M. Agreement between left ventricular ejection fraction assessed in patients with gated IQ-SPECT and conventional imaging. J Nucl Cardiol. 2020 Oct;27(5):1714-1724.

Ljungberg M, Strand SE. A Monte Carlo program for the simulation of scintillation camera characteristics. Comput Methods Programs Biomed. 1989 Aug;29(4):257-72.

Mansoor MR, Heller GV. Gated SPECT imaging. Semin Nucl Med. 1999 Jul;29(3):271-8.

Onoguchi, Masahisa & Konishi, Takahiro & Shibutani, Takayuki & Matsuo, Shinro & Nakajima, Kenichi. (2016). Technical Aspects : Image Reconstruction. Annals of Nuclear Cardiology. 2. 68-72. 10.17996/ANC.02.01.68.

Pahlm O, Wagner G (ed). Multimodal cardiovascular imaging: Principles and clinical applications. 2011, The McGraw-Hill Companies, Inc.

Paul AK, Nabi HA. Gated myocardial perfusion SPECT: basic principles, technical aspects, and clinical applications. J Nucl Med Technol. 2004 Dec;32(4):179-87; quiz 188-9.

Platts EA, North TL, Pickett RD, Kelly JD. Mechanism of uptake of technetium-tetrofosmin. I: Uptake into isolated adult rat ventricular myocytes and subcellular localization. J Nucl Cardiol. 1995 Jul-Aug;2(4):317-26. doi: 10.1016/s1071-3581(05)80076-5. Erratum in: J Nucl Cardiol 1995 Nov-Dec;2(6):560.

Ravishankar S, Ye JC, Fessler JA. Image Reconstruction: From Sparsity to Data-adaptive Methods and Machine Learning. Proc IEEE Inst Electr Electron Eng. 2020 Jan;108(1):86-109.

Salerno M, Sharif B, Arheden H, Kumar A, Axel L, Li D, Neubauer S. Recent Advances in Cardiovascular Magnetic Resonance: Techniques and Applications. Circ Cardiovasc Imaging. 2017 Jun;10(6):e003951.

Saraste A, Barbato E, Capodanno D, Edvardsen T, Prescott E, Achenbach S, Bax JJ, Wijns W, Knuuti J. Imaging in ESC clinical guidelines: chronic coronary syndromes. Eur Heart J Cardiovasc Imaging. 2019 Nov 1;20(11):1187-1197.

Segars WP, Sturgeon G, Mendonca S, Grimes J, Tsui BM. 4D XCAT phantom for multimodality imaging research. Med Phys. 2010 Sep;37(9):4902-15.

Severino P, D'Amato A, Pucci M, Infusino F, Adamo F, Birtolo LI, Netti L, Montefusco G, Chimenti C, Lavalle C, Maestrini V, Mancone M, Chilian WM, Fedele F. Ischemic Heart Disease Pathophysiology Paradigms Overview: From Plaque Activation to Microvascular Dysfunction. Int J Mol Sci. 2020 Oct 30;21(21):8118.

Sirajuddin A, Mirmomen SM, Kligerman SJ, Groves DW, Burke AP, Kureshi F, White CS, Arai AE. Ischemic Heart Disease: Noninvasive Imaging Techniques and Findings. Radiographics. 2021 Jul-Aug;41(4):990-1021.

Trägårdh E, Hesse B, Knuuti J, Flotats A, Kaufmann PA, Kitsiou A, Hacker M, Verberne HJ, Edenbrandt L, Delgado V, Donal E, Evardsen T, Galderisi M, Habib G, Lancellotti P, Nieman K, Rosenhek R; EACVI; Agostini D, Gimellli A, Lindner O, Slart R, Ubleis C; EANM. Reporting nuclear cardiology: a joint position paper by the European Association of Nuclear Medicine (EANM) and the European Association of Cardiovascular Imaging (EACVI). Eur Heart J Cardiovasc Imaging 2015 Mar;16(3):272-9.

Van Audenhaege K, Van Holen R, Vandenberghe S, Vanhove C, Metzler SD, Moore SC. Review of SPECT collimator selection, optimization, and fabrication for clinical and preclinical imaging. Med Phys. 2015 Aug;42(8):4796-813.

Verberne HJ, Acampa W, Anagnostopoulos C, Ballinger J, Bengel F, De Bondt P, Buechel RR, Cuocolo A, van Eck-Smit BL, Flotats A, Hacker M, Hindorf C, Kaufmann PA, Lindner O, Ljungberg M, Lonsdale M, Manrique A, Minarik D, Scholte AJ, Slart RH, Trägårdh E, de Wit TC, Hesse B; European Association of Nuclear Medicine (EANM). EANM procedural guidelines for radionuclide myocardial perfusion imaging with SPECT and SPECT/CT: 2015 revision. Eur J Nucl Med Mol Imaging. 2015 Nov;42(12):1929-40.

Printed by Media-Tryck, Lund 2023 NORDIC SWAN ECOLABEL 3041 0903

LUND UNIVERSITY

FACULTY OF MEDICINE

Department of Translational Medicine
Clinical Physiology and Nuclear Medicine

ISBN 978-91-8021-384-4
ISSN 1652-8220